# SIMULATION OF SOLAR GAINS THROUGH EXTERNAL SHADING DEVICES

D.K.Alexander[*], K.A.Ku Hassan[†], P.J.Jones[*]
[*]Welsh School of Architecture
Bute Building, Cardiff
CF1 3AP, U.K.
[†]School of Housing, Building, and Planning
Universiti Sians Malaysia
Penang, Malaysia

## ABSTRACT

The effectiveness of simple shading devices in reducing the direct, diffuse and ground reflected components of solar radiation has been measured and compared to simulation predictions of the same. The simulation results were found to be very sensitive to the value assumed for ground reflectance, and to the level of detail of the geometrical modelling of the shading devices. The best agreement total incident radiation was within 3% over the course of a day.

## INTRODUCTION

As part of a recent doctoral investigation [Hassan], the effectiveness of simple shading devices (overhangs and side-fins) in reducing solar gains were tested. An intent of the investigation was to quantify the reduction of the diffuse and reflected components of solar gains, as well as of the direct component. Although the direct solar component can be often be easily eliminated, the diffuse sky and ground reflected components can be significant in some climates [Jones]. To achieve the investigations aims, a limited measurement exercise was to be extended by simulation methods.

The initial results from investigations into the accuracy of simulation codes [Lomas] suggested shortcomings in solar calculation algorithms as one of the possible sources of discrepancies between models. Therefore, testing and comparison was felt necessary to demonstrate the ability of the modelling methodology to adequately predict the performance of the solar shading devices.

To provide data for such a test, a model window aperture was constructed, within which area the incident solar radiation could be accurately measured and dissaggregated into direct, diffuse and reflected components. Several types of external shading devices were applied to this aperture. The measurements of the solar radiation components reaching the aperture were then compared to predictions of the same, using a dynamic thermal model (HTB2).

## MEASUREMENT

The model window was an unglazed aperture only, thus the measurements made no attempt at determining solar gains to a space, transfer coefficients of glazing, or of cavity losses and back-reflectance.

The measurements of solar irradiance to the model window aperture were made using a rig containing five Kipp and Zonen solarimeters mounted on a horizontal bar which could be moved vertically across the opening. This provided 25 measurement points within the opening, as shown in figure 1. A complete scan could be made in approximately 1 minute; because of the time required for a scan, measurements were made only under stable sky conditions. To achieve even this scan time, the dwell time at each station was less than the recommended settling time of the solarimeters used. To correct for this, an exponential step-change response factor was applied during the data processing to extrapolate a the final “steady” condition. Trial measurements indicated a good uniformity in measured incident radiation across the aperture for the unshaded case, with the individual stations matched to less than 1% across the aperture. For a shaded case, the shadow band caused by the shading device could be adequately discerned, as illustrated in figure 2.

The rig was mounted vertically and could be orientated to any heading. It was located on the roof of the Welsh School of Architecture, Cardiff (Latitude ~52N) which, although in an urban location, was above surrounding buildings and provided a clear horizon. The roof on which the measurement rig was mounted was covered with a reflective bitumen coating, whilst the view beyond was a mixture of green-belt parkland and low (<3 storey) buildings.

The unshaded vertical, and the global and diffuse horizontal solar irradiance, were measured locally and coincidentally with the solar irradiance incident to the aperture.

Through the use of shading discs and cups applied to the solarimeters on the rig, as illustrated in figure 3, the components of the incident solar radiation could be estimated. The differences in the measured irradiance between configurations provided the estimates of the components. Thus for instance, configuration A of figure 3 measures the global irradiance while configuration C would provides a measure of direct and diffuse sky vault irradiance only, excluding the ground reflected component. The ground reflected component is calculated from the difference between the results for C and A.

Each of these obscuration devices would be used in turn, in each measurement run. A full measurement set could be made only under stable sky conditions; e.g. clear sky or full overcast. The configurations used allowed at least two independent estimates to be made for each component, summarised table 1.

Table 1 also contains an estimate of the measurement accuracy attained for each component, allowing for the accuracy of the solarimeter, the placement of the obscuration devices, and the signal processing involved.

Table 2 shows sample results for a measurement run of an unshaded south facing aperture under a June clear sky. The values quoted are the incident solar radiation averaged over the aperture. The relative importance of the solar components can be easily seen. As would be expected in UK conditions the diffuse component is relatively small, the direct beam dominant.

## SIMULATION

Simulations were carried out using the dynamic thermal model HTB2. This simulation code was developed in the Welsh School of Architecture and has been reported previously [Lewis and Alexander]. It is in use in a number of institutions, and was included in the recent IEA comparison of thermal models [Lomas].

HTB2 was used in this investigation primarily due to in-house familiarity, although its flexibility and particular features offered several advantages. In particular the HTB2 approach to the description of shading devices is novel. Rather than containing a fixed algorithm and input based on a geometrical description, HTB2 accepts a description of the sky vault as effectively "seen" by a opening or surface; a shading mask. This mask describes the effective transmission factor of the (general) solar radiation from a sector of the sky to the window opening. These sectors are described in 10 degree steps and cover the whole hemisphere of the sky. This approach is advantageous in that the mask can be estimated from a number of sources, including theoretical calculation or fish-eye view photographs. The mask can also include the effect of external obstructions, (e.g. walls and vegetation) as well as local devices.

A shading device may obscure totally the solar radiation from certain sectors, partially or not at all in others, as illustrated in figure 4. In application, the attenuation of the direct beam during calculation is determined from the known position of the sun in the sky vault. The diffuse sky component is estimated from the integration of all the sectors "visible" to the surface. In the current implementation of HTB2 (version 1.10), the ground reflected component is not considered to be affected by a shading device.

An example visualisation of a complex HTB2 shading description is shown in figure 5. The light sectors have little obstruction to solar radiation, the black sectors allow no solar gain from that direction. In application this data is recorded as a numerical table, 36x9 entries describing the transmission factor for each sector.

Other than the calculation of the effect of shading, the solar algorithms used in HTB2 are those commonly found in other similar codes. The algorithms used for unshaded beam, and diffuse solar components are based on those documented by [Page] and on those presented by [Hoyt]. An isotropic sky distribution is assumed for the diffuse solar component.

The configuration of HTB2 as used in this investigation excluded its' thermal calculations, thus only the solar irradiance to the model window area was calculated. No glazing, framing, or cavity losses were assumed or accounted for. Values quoted for the simulations are the incident solar radiation averaged over the entire aperture.

Simulations of the solar irradiance on the window aperture were carried out using the specific geometry of the test rig, and the concurrently measured global and diffuse horizontal solar irradiance.

## COMPARISONS : UNSHADED CASES

The initial comparison of measurement and prediction for the unshaded case was disappointing;

for instance peak global irradiance was measured at 606 W/m$^2$ but predicted as 539 W/m$^2$. It was determined that the simulation results were highly dependant on the value of adjacent ground reflectance specified, as shown in table 3. Altering the assumed ground reflectance factor from the usual default value of 0.2 through to 0.4 produced a change in predicted peak incident radiation from 539 to 625 W/m$^2$. The measurement site was less than ideal, as it contained a significant expanse of a reflective bitumen coating. The albedo of this material was measured as 0.40 ± 0.04. The ground visible from the test window included a considerable expanse of this material, but also included nearby buildings, roads and parkland, for which a reflectance of 0.2 is often used. The best agreement between the predictions and measurements for the unshaded case were achieved for an average ground reflectivity of 0.35. This was considered a reasonable value given the mix of environments as indicated above, and this "calibrated" value was used for the rest of the measurement/simulation comparisons with shading devices. This was the only calibration step required to achieve reasonable agreement. The agreement achieved over a complete day was better than 7 W/m$^2$ or ~2% on individual hours, and within 35 Wh/m$^2$ (~1%) over the course of a day. Without correcting for the ground reflectance conditions, the predictions were only within 58 W/m$^2$ and 523 Wh/m$^2$ for the hourly and total day irradiance respectively, thus significantly under-predicting solar gains. This highlights the importance of the value of ground reflectance assumed in simulation assessments.

## COMPARISONS : SHADED CASES

Consideration of a simple horizontal projection, with an overhang extent of 0.5m and a width of 1.2m, was next undertaken. As shown in figure 6, prediction agreement was found to be acceptable at midday, but less so at the start and end of the day. Unlike the unshaded case, there is not a simple offset that may be attributed to a incorrect parameter such as ground reflectance.

The shading description used for these initial simulation tests was calculated using the geometrically simple "infinite extent" assumption; a typical assumption often made in simulation codes. In this simplification only the vertical shadow angle is calculated; the obstruction is considered to have an infinite extent horizontally, and so there is no allowance for edge effects. In practice there would be greater solar penetration past the device for oblique solar angles, e.g. morning and evening for southern facing devices, and this is indeed what has been found.

Alternative calculation procedures were sought to allow for these edge effects. General shading algorithms were found in [Feuerstein], which accounted fully for the geometry of the problem. These algorithms were adapted and the shading masks describing the shading of the rigs recalculated.

Although the alterations made to the shading description was subtle, the agreement, as shown in table 4 and figure 6 is much improved. The hourly predicted solar irradiances are within 3%, and often within 1% of the measurements. Over the course of a day, the predicted total irradiance is within 31 Wh/m$^2$ (~2%) as opposed to within 156 Wh/m$^2$ for the simpler geometric assumption. Note that due to the effect of the shading device, the observed irradiance values are considerably less that the preceding case, Both measurements were undertaken in similar blue-sky conditions.

Due to the dismissal of edge effects, the simpler geometric shading model overestimates the efficacy of the shading device. For the conditions of these tests this overestimate was found to be ~150 Wh/m$^2$/day, a significant error which could lead to an error in predicted peak room temperature or cooling load.

Similar results were found when considering vertical shading devices; e.g. side-fins. As seen in figure 7, the predictions of solar irradiance using the simpler "infinite-extent" geometric model of the shading device does not match the measurements well. Again edge effects are important and the predictions using the more detailed geometric shading model of Feuerstein provide a much more favourable comparison. Table 5 contains the hourly comparison data. The more detailed shading description provides an agreement in hourly value to within 15 W/m$^2$ and in total daily irradiance to 135 Wh/m$^2$. The infinite extent assumption again overestimate the efficacy of the device over the course of a day, calculating a total irradiance 1129 Wh/m$^2$ less than that measured.

"Egg-crate" devices combine repeated overhangs and side fins. This removes the important of edge effects and the Feuerstein and the infinite extent models of shading provide similar shading descriptions. Either then would produce the agreement shown figure 8 and table 6. In this case the simulations were within 6 W/m$^2$ and 21 Wh/m$^2$ for the hourly and total day irradiance respectively.

## COMPARISONS: SOLAR COMPONENTS

The prediction of global irradiance could match measurements whilst being incorrect in the relative contibution of its' components. For those predictions made using the Feuerstein model, this does not seem to be the case, the accuracy of the predictions does extend to the individual components. Figures 9 through 12 shown the direct beam and ground reflected solar components (as a proportion of the hourly global irradiance) for the unshaded and the three shaded cases considered. The agreement between predictions and measurement is good, within 10% for the shaded cases. Those errors that occur cannot be resolved to be attributable to the simulation of measurement method; for instance the comparisons show a small amount of measured direct solar even at mid-day, where in theory (and in experience) there should be none. This is felt to reflect the accuracy of the component measurement path; the simulation values are within the measurement error bands. There is therefore a useful degree of accuracy in the prediction of the components of solar gains past a shading device, and so the simulation method is viable for use in optimising shading.

It is noted that the calculation of the effect of a shading devices as used in HTB2 takes no account of reflection off the device itself, nor of the attenuation of the ground reflected component. This may limit the accuracy of the application to devices such as "egg-crate" shades. This is being reviewed for modification in later version of the code.

## CONCLUSIONS

The modelling method was shown to be capable of accurate prediction of effect of external shading devices on solar energy incident on windows. The primary requirements for agreement with measurements was the correct specification of adjacent ground reflectance, and the use of a detailed geometric model of the shading devices, which correctly accounted for edge effects. Using the infinite extent assumption for shading devices leads to significant errors and overestimates the effect of the device in reducing solar gains to spaces.

The simulations were found to be able to predict unshaded solar irradiation to a window area to within 1.5% though a day, and to predict shaded solar irradiation to the window area to within 3%. Using incorrect values for ground reflectance, or using the "infinite-extent" shading model could lead to errors in the prediction of solar irradiance of over 10%. Additionally, the "infinite-extent" model significantly over-estimates the effectivness of shading devices.

The prediction of the components of shaded solar irradiance, the direct beam, diffuse and ground reflected components, was to within 10% when using the detailed geometrica shading model.

The confidence in the use of the novel shading description used in HTB2 was increased, allowing its use in the optimisation of external shading devices in general.

## ACKNOWLEDGEMENTS

The authors thank Mr S Lannon for his help during the construction of the measurement equipment.

## REFERENCES

Feuerstein, G.R., "General Case Analysis of Shadow Area Equations for Window Overhang, Sidefins and Parapets", ASHRAE technical paper 2549, ASHRAE Transactions 1986.

Hoyt,D.V., "A Model for the Calculation of Solar Global Insolation", Solar Energy 21, 1973, pp27-35.

Jones, P.J, Alexander, D.K, and Rahman, A.K, "Evaluation of the Thermal Performance of Low-Cost Tropical Housing", Proceedings BS'93, IBPSA, p 137-143, 1994.

Ku Hassan, K.A., "The Application of Solar Shading Devices for Buildings in Hot Humid Climates, with Special Reference to Malaysia", PhD thesis, University of Wales College of Cardiff, May 1996.

Lewis P.T, and Alexander, D.K. "HTB2: A Flexible Model for Dynamic Building Simulation", Building and Environment 25, no. 1, 1990.

Lomas, K., Eppel, H., Martin, C., Bloomfield, D., "Empirical Validation of Thermal Building Simulation Programs Using Test Room Data", IEA 21C/12B Final Report. 1994.

Page, J.K., "A Meteorological Database System for Architectural and Building Engineering Designers; Handbook Volume II", EPSRC Publication, grant GR/B/40219, 1984

| Solar Component | Determined from Configurations: | Estimated Error |
|---|---|---|
| Global | A | 5% |
| Direct | (C-E) or (A-C) | 8% |
| Diffuse | E or (D-B) | 6% |
| Ground Reflectance | B or (A-C) | 10% |

Table 1 Estimate of solar components from sensor configurations (cf figure 3) and their associated errors

**Solar Radiation Incident on Window W/m$^2$**

| Time | Global Vertical | Direct Beam | Diffuse Vault | Ground Reflection |
|---|---|---|---|---|
| **9** | 244 | 112 | 49 | 81 |
| **10** | 363 | 207 | 51 | 105 |
| **11** | 479 | 297 | 57 | 125 |
| **12** | 564 | 367 | 56 | 141 |
| **13** | 606 | 400 | 55 | 151 |
| **14** | 583 | 385 | 46 | 152 |
| **15** | 511 | 317 | 46 | 148 |
| **16** | 370 | 189 | 44 | 137 |
| **17** | 187 | 28 | 45 | 144 |

Table 2: Sample measurement result for an unshaded case

**Solar Radiation Incident on Window W/m$^2$**

| Time (hr) | Measured | Predicted: ground refl. = 0.2 | = 0.3 | = 0.35 | = 0.4 |
|---|---|---|---|---|---|
| **9** | 243 | 189 | 211 | 222 | 233 |
| **10** | 363 | 316 | 345 | 361 | 375 |
| **11** | 479 | 420 | 456 | 473 | 491 |
| **12** | 564 | 503 | 544 | 564 | 584 |
| **13** | 606 | 539 | 583 | 603 | 625 |
| **14** | 583 | 519 | 561 | 583 | 605 |
| **15** | 511 | 445 | 488 | 509 | 530 |
| **16** | 370 | 314 | 352 | 370 | 389 |
| **17** | 187 | 138 | 169 | 186 | 202 |

Table 3: Comparison of unshaded solar irradiance to prediction with different assumed ground reflectance

**Solar Radiation on Window W/m$^2$ using Horizontal Shading**

| Time | Measured | Predicted: using Infinite extent | using Feuerstein |
|---|---|---|---|
| **9** | 122 | 89 | 109 |
| **10** | 153 | 117 | 152 |
| **11** | 146 | 138 | 145 |
| **12** | 159 | 156 | 159 |
| **13** | 170 | 165 | 169 |
| **14** | 167 | 176 | 167 |
| **15** | 179 | 159 | 175 |
| **16** | 183 | 145 | 180 |
| **17** | 146 | 124 | 138 |

Table 4 Comparison of total solar irradiance past horizontal 0.5m overhang projection for measured and predicted cases.

**Solar Radiation on Window W/m$^2$**
**using Vertical Shading**

| Time | Measured | Predicted: using Infinite extent | using Feuerstein |
|---|---|---|---|
| **9** | 206 | 94 | 170 |
| **10** | 307 | 123 | 269 |
| **11** | 408 | 219 | 403 |
| **12** | 549 | 446 | 542 |
| **13** | 586 | 521 | 581 |
| **14** | 518 | 416 | 513 |
| **15** | 429 | 245 | 423 |
| **16** | 307 | 150 | 278 |
| **17** | 162 | 129 | 158 |

Table 5 Comparison of total solar irradiance past vertical 0.5m side-fin projection for measured and predicted cases.

**Solar Radiation on Window W/m$^2$**
**using "Egg -crate" shading**

| Time | Measured | Predicted: using Feuerstein |
|---|---|---|
| **9** | 88 | 83 |
| **10** | 116 | 111 |
| **11** | 134 | 131 |
| **12** | 156 | 148 |
| **13** | 165 | 158 |
| **14** | 163 | 158 |
| **15** | 158 | 153 |
| **16** | 133 | 139 |
| **17** | 108 | 119 |

Table 6 Comparison of total solar irradiance past 0.5m "Egg-crate" projections for measured and predicted cases.

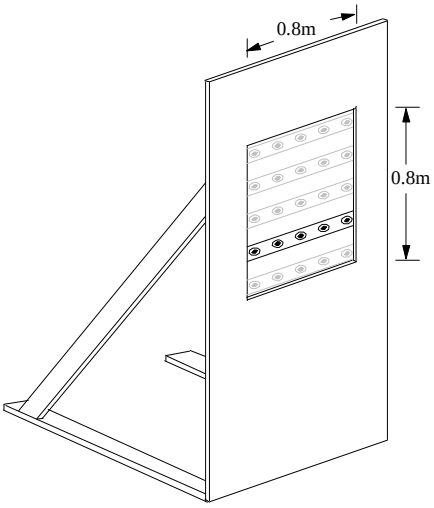


Figure 1 - Sketch of test window aperture and measurement rig, showing scanning

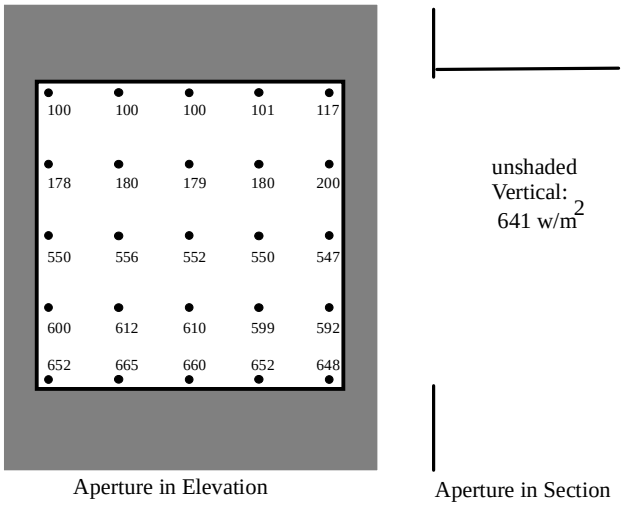


Figure 2 Irradiance distribution measured over window aperture; Overhang case: South orientation:14:00:

positions.

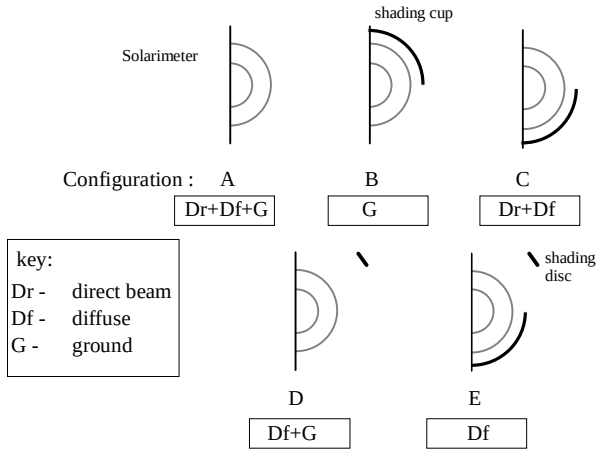


Figure 3 - Solarimeter cell masking configurations

July. Irradiance in W/m$^2$

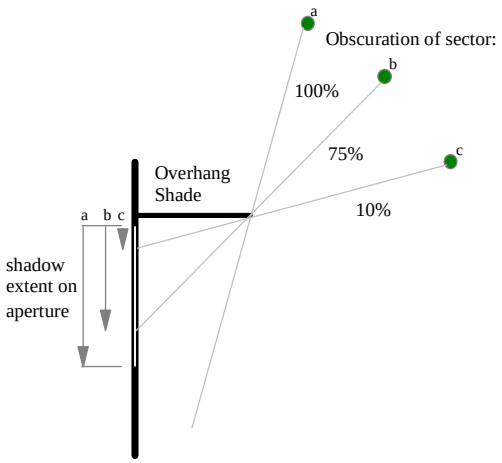


Figure 4 Principles of an HTB2 shading mask

Figure 5 Example visualisation of an HTB2 shading mask, containing overhang, sidefin, and site obstructions.

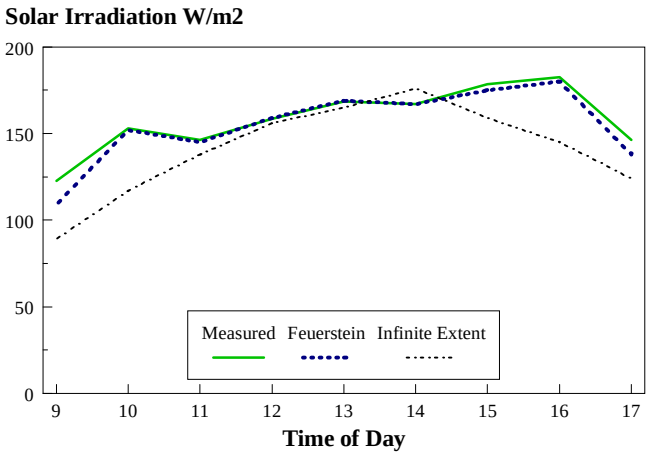


Figure 6 - Comparison of measurement and prediction of total solar irradiance for the horizontal overhang shaded case.

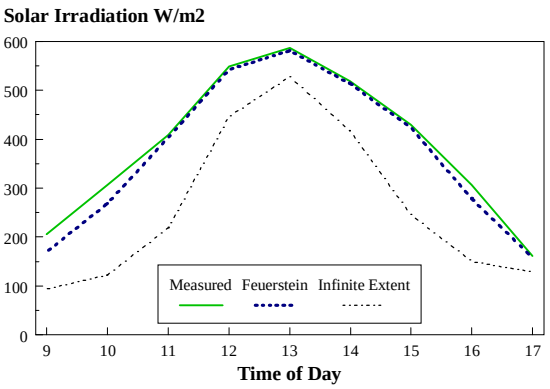


Figure 7 Comparison of measurement and prediction of total solar irradiance for the vertical side-fin shaded case.

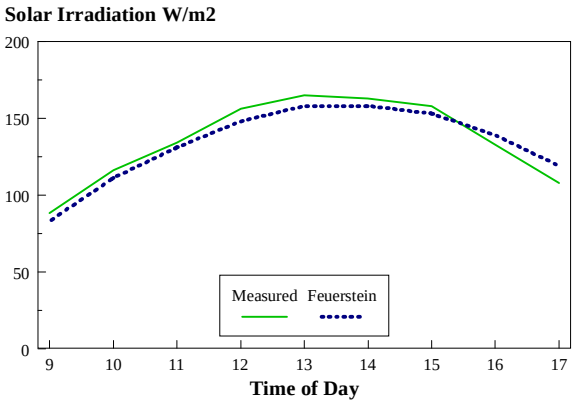


Figure 8 Comparison of measurement and prediction of total solar irradiance for the "egg-crate" shaded case.

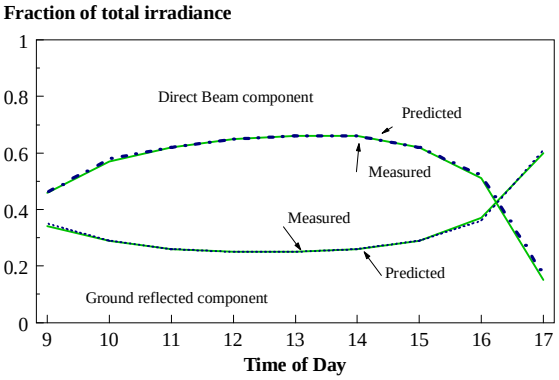


Figure 9 Comparison of measurement and prediction of the solar components for the unshaded case.

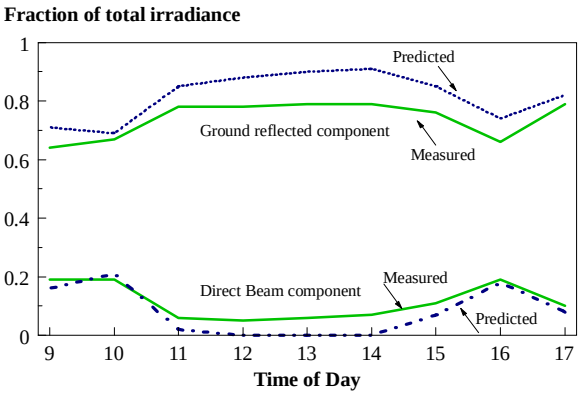


Figure 10 Comparison of measurement and prediction of the solar components for the horizontal overhang shaded case.

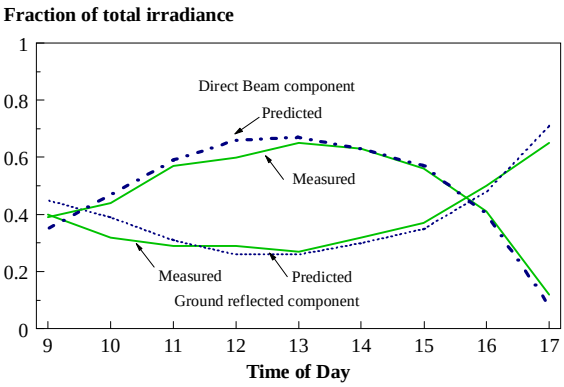


Figure 11 Comparison of measurement and prediction of the solar components for the vertical side-fin shaded case.

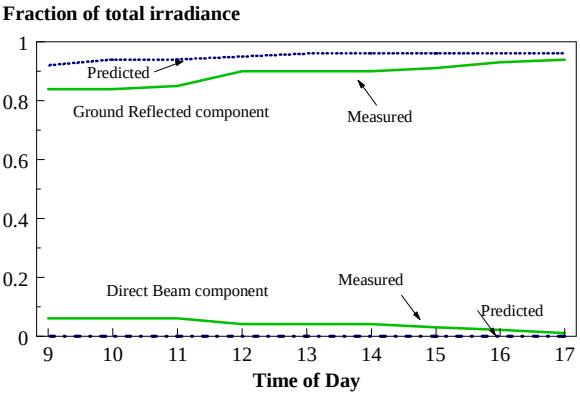


Figure 12 Comparison of measurement and prediction of the solar components for the "egg-crate" shaded case.